

# A STUDY OF TOPOLOGICAL ASSESSMENT OF HEXANE PARA-LINE GRAPHS WITH THE ANALYSIS OF THE CHEMICAL COMPOSITION

Mukhtar Ahmad<sup>1</sup>, Ather Qayyum<sup>2</sup>, Muhammad Maaz<sup>3</sup>, Muhammad Muawwaz<sup>3</sup> and Siti Suzlin Supadi<sup>2</sup>

<sup>1</sup> Department of Mathematics, Khawja Fareed University of Engineering and Information Technology Rahim Yar Khan, Pakistan.

<sup>2</sup> Institute of Mathematical Sciences, Universiti Malaya, Malaysia .

<sup>3</sup> Institute of Southern Punjab Multan, Pakistan.

Correspondence Author: dratherqayyum@um.edu.my

Correspondence Author: itxmemukhtar@gmail.com

**Abstract:** Topological indices (TIs) are widely utilized as molecular descriptors in the development of quantitative structure-activity relationships (QSAR), quantitative structure-property relationships (QSPR) and quantitative structure-toxicity relationships (QSTR). Molecular descriptors play a crucial role in mathematical chemistry, particularly in investigations involving quantitative structure-property relationships (QSPR) and quantitative structure-activity relationships (QSAR). A topological index represents a numerical mapping of a molecule's structure. It is employed to characterize the physicochemical properties of specific substances and remains unchanged under graph transformations. The focus of our study is to analyze the chemical composition of pentacene. Our research developed into various indices, including the general randic connectivity index, the first and second multiple zagreb indices, the first general zagreb index, the atomic bond connectivity index, the hyper zagreb index, the geometric arithmetic index, the general sum-connectivity index, the fifth class of geometric arithmetic indices for hexane para-line graphs of multi-pentacene, linear pentacene and linear  $[n]$ -pentacene.

**Keywords:** Graphs of hexane para-line, topological indices, pentacene, nanostructures, linear pentacene.

## 1. INTRODUCTION AND PRELIMINARIES

All substances molecule possesses qualities, both chemical and physical and certain may also exhibit physiologically active characteristics. Several pharmaceutical companies are really hunting for novel antibacterial chemicals. For this reason, hundreds of compounds are examined, however costly examinations for biology. In order to circumvent such issue, additional methods for investigating potential antibiotics employ the relationship between structural features and biological activity or features of chemical and physical nature. Topological indices or molecular descriptors, provide insights into the physicochemical properties of molecules. They are valuable tools for understanding and explaining the characteristics of chemical compounds. Several graph invariants have been created in recent years and have been used in many academic fields such as structural chemistry, environmental chemistry, theoretical chemistry, pharmacology and toxicology. Because of the substantial industrial need, researchers are urged to study topological indices. More than 400 topological indexes have been opened a consequence of research. Chemical compounds topological structures and chemical characteristics are tightly related, since each compound's shape is critical to

determining its functionality. Topological indices are often used in multilinear regression modelling, chemical documentation, drug design, QSAR/QSPR modelling and database selection. Molecular descriptors are utilized to describe the physicochemical properties of molecular structures. These descriptors can be classified into three main types degree-based indices [1-5], distance-based indices [6-11] and spectrum-based indices [12-15]. Studies that have been documented in the literature (see [16-18]) use indicators that are based on both distances and degrees.

Due to pentacene's important functions in both electrical devices and organic solar cells, a popular hydrocarbon semiconductor, it is necessary to optimise organic solar cells for less expensive energy sources[19]. The georgia institute of technology researchers have developed method to produce portable artificial solar cells. Pentacene has been shown to be a very efficient means of converting sunlight into energy. In contrast to other materials, pentacene functions well as a semiconductor due to its crystalline properties. Pentacene's relevance motivated us to do topological study on it and as a result, we have made several important discoveries that could be helpful for analysing pentacene's physical and chemical characteristics See [20, 21] for further topological research on pentacene.

Hexane is an organic compound classified as a straight-chain alkane containing six carbon atoms, represented by the molecular formula  $C_6H_{14}$ . It is characterized as a colorless and odorless liquid in its pure form, with a boiling point of approximately 69 celsius (156 farhenheit). Hexane is commonly employed as a non-polar solvent due to its relative safety, low reactivity, afford ability and ease of evaporation. Additionally, hexane plays a significant role as a constituent in gasoline. Sometimes, the term "hexane" refers to a mixture consisting primarily (> 60 percent) of hexane, along with varying amounts of isomeric compounds such as 2-methyl pentane, 3-methyl pentane and possibly smaller quantities of non-isomeric alkanes (cyclo) of  $C_5$ ,  $C_6$  and  $C_7$ . Hexane is preferred in large-scale operations where a single isomer is not required, such as in the context of cleaning solvents or chromatography procedures. Hexane is a refined crude oil used in various industrial applications, including adhesives, roofing materials, leather products, cooking oil extraction, degreasing, cleaning, and textile manufacturing. It is commonly used in the US for soybean oil extraction, causing controversy due to FDA lack of regulation. In laboratories, it is used to extract grease and oil contaminants for analysis. Hexane is also used in reactions involving strong foundations, like the creation of organolithium compounds like butyllithium. Hexane serves as a non-polar solvent in chromatography, where it finds widespread use. However, it's important to note that hexane may contain impurities in the form of higher alkanes, which have similar retention times as the solvent itself. Consequently, fractions containing hexane may also contain these impurities, which can lead to the presence of alkanes in solid compounds obtained from chromatographic analysis, potentially interfering with the accuracy of the analysis.

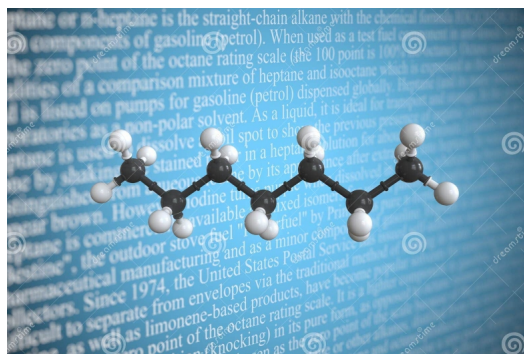


FIGURE 1. fig

Hexane's acute toxicity is relatively low. In halation of n-hexane or hexane n at a concentration of 5000 parts per million (ppm) for a duration of just 10 minutes can result in significant vertigo. Exposure to concentrations ranging from 2500 to 1000 ppm for 12 hours can lead to symptoms such as fatigue, loss of appetite, drowsiness and tingling or numbness in the extremities. In the range of 2500 to 5000 ppm, it can cause cold pulsation in the extremities, muscle weakness, headache, loss of appetite and blurred vision. Prolonged occupational exposure to elevated levels of n-hexane or hexane n has been associated with neurotoxicity among workers in printing presses, as well as peripheral neuropathy in auto mechanics in the United States, Europe, Asia and North America, particularly in furniture and shoe factories. In certain circumstances, n-hexane is permitted for various applications such as serving as a denaturant for alcohol and as a cleaning agent in the textile, furniture and leather industries. Similar to gasoline, hexane is highly volatile and poses a risk of explosion. Figure 1(a) depicts the molecular graph and its structure of hexane . Further more, figure 2(b) and (c) exhibit the hexane para-line graphs derived from the molecular plot of hexane. now figure are;

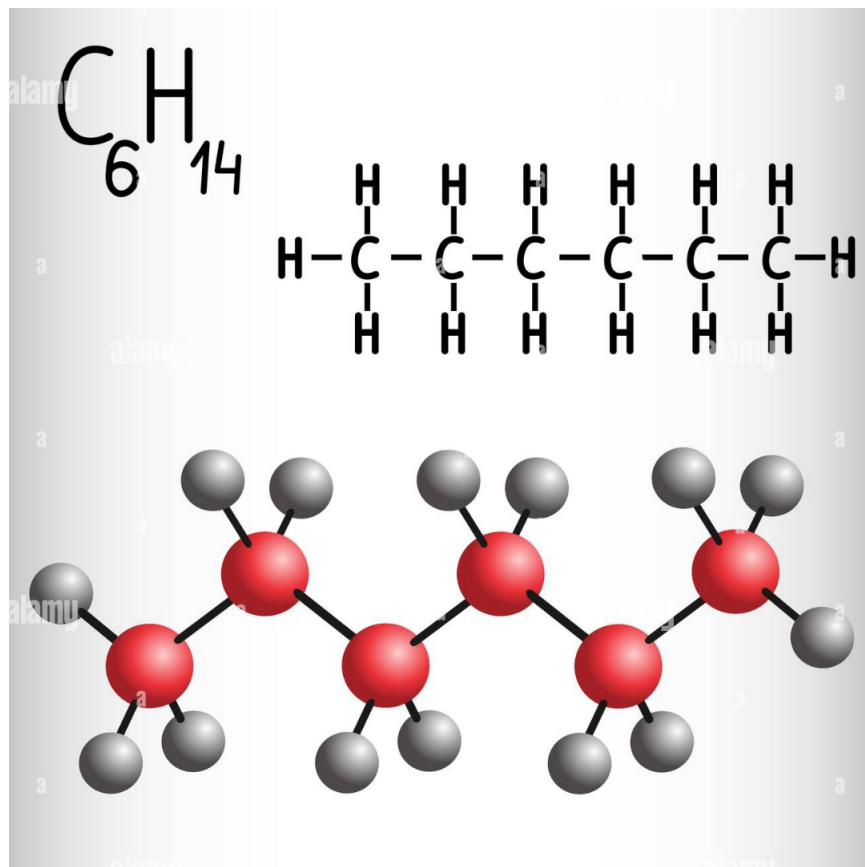


FIGURE 2. fig

The definition of the generic randic connection index  $G$  is [12].

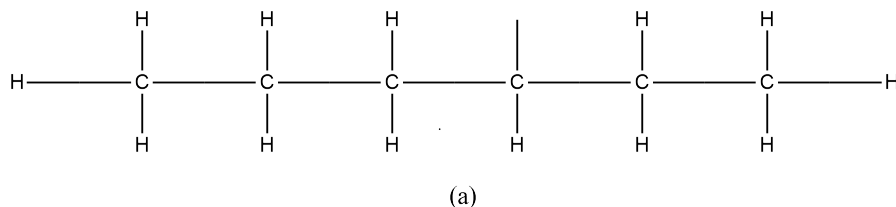


FIGURE 3. (a)Molecular structure of hexane

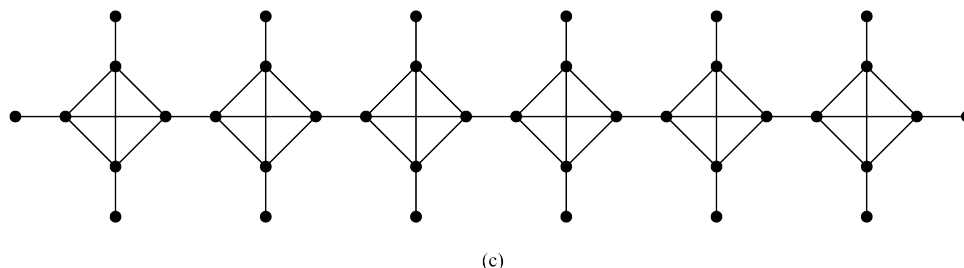
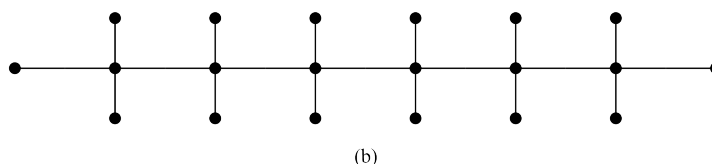


FIGURE 4. (b) Molecular graph of hexane, (c) Tera-line graph of hexane

$$R_{\alpha}(G) = \sum_{x_1 x_2 \in E(G)} (d_{x_1} d_{x_2})^{\alpha} \quad (1)$$

The first universal zagreb index was presented by Li and Zhao[22]:

$$M_{\alpha}(G) = \sum_{x_1 \in V(G)} (d_{x_1})^{\alpha} \quad (2)$$

The the general sum connectivity index of the  $G$  chart was introduced in 2010 [23]:

$$\chi_{\alpha}(G) = \sum_{x_1 x_2 \in E(G)} (d_{x_1} + d_{x_2})^{\alpha} \quad (3)$$

The index (ABC) was proposed by Estrada [24]. It is expressed as follows for a graph  $G$ :

$$ABC(G) = \sum_{x_1 x_2 \in E(G)} \sqrt{\frac{d_{x_1} + d_{x_2} - 2}{d_{x_1} d_{x_2}}} \quad (4)$$

The geometric-arithmetic index (GA) was introduced by Vukicevic and Furtula [25]. It is denoted as  $GA$  and is defined as follows for a graph  $G$  resently A. Asghar et.al[31]:

$$GA(G) = \sum_{x_1 x_2 \in E(G)} \frac{2\sqrt{(d_{x_1} d_{x_2})}}{(d_{x_1} + d_{x_2})} \quad (5)$$

Ghorbani et al. [26] described another index belonging to the 4th class of indices, denoted as (ABC), which is defined as follows recently Zaib Hassan Niazi et.al[32]:

$$ABC_4(G) = \sum_{x_1 x_2 \in E(G)} \sqrt{\frac{d_{S_1} + S_{x_2} - 2}{S_{x_1} S_{x_2}}} \quad (6)$$

Graovac et al. [27] introduced a fifth class of geometric-arithmetic indices denoted as  $GA_5$ , which is defined as follows:

$$GA_5(G) = \sum_{x_1 x_2 \in E(G)} \frac{2\sqrt{(S_{x_1} S_{x_2})}}{(S_{x_1} + S_{x_2})} \quad (7)$$

Established the hyper-zagreb index in 2013 as follows recently Mukhtar Ahmad et.al[33]:

$$HM(G) = \sum_{x_1 x_2 \in E(G)} (d_{x_1} + d_{x_2})^2 \quad (8)$$

In 2012, Ghorbani and Azimi introduced two new types of zagreb graph indices. The first is the first multiple zagreb index, denoted as  $PM_1(G)$ . The second multiple zagreb index is used, denoted as  $PM_2(G)$ . Additionally, the first and second zagreb polynomials,  $M_1(G, p)$  and  $M_2(G, p)$ , respectively, are characterised as recently Mukhtar Ahmad et.al[34]:

$$PM_1(G) = \prod_{x_1 x_2 \in E(G)} (d_{x_1} + d_{x_2}) \quad (9)$$

$$PM_2(G) = \prod_{x_1 x_2 \in E(G)} (d_{x_1} \times d_{x_2}) \quad (10)$$

$$M_1(G, p) = \sum_{x_1 x_2 \in E(G)} P^{(d_{x_1} + d_{x_2})} \quad (11)$$

$$M_2(G, p) = \sum_{x_1 x_2 \in E(G)} P^{(d_{x_1} \times d_{x_2})} \quad (12)$$

## 2. TOPOLOGICAL INDEX OF HEXANE PARA-LINE GRAPHS

For an index that Schultz offered, Ranjini created the independent relations. Under the watchful eye of the Schultz index, these researchers looked at the subdivision of a number of graphs, including helm, ladder, tadpole and wheel [28]. They also looked at the ladder, tadpole and wheel hexane para-line graphs under the zagreb index [29]. In 2015, Xu and Su conducted an analysis of two indices specific to ladder, tadpole and wheel graphs constructed using hexane para-line graphs and named the total connectivity index of the sum and the co-index [30]. Nadim et al. calculated the atomic bond connectivity index and fifth class of geometric arithmetic indices for hexane para-line tadpole, wheel and ladder graphs. They also investigated several other indices, including randic general connectivity index, first zagreb general index, summation general connectivity index, atomic bond connectivity index, geometric arithmetic index, fifth class of geometric arithmetic indices, hyper zagreb index, the first and second multiple zagreb index for a hexane para-line graphs of linear [n]-pentacene and multiple pentacene., lattice plot in nanotorus  $TUC_4C_8[p, q]$  and 2D nanotube .

In our study, we computed various indices, including randic general connectivity index, first zagreb general index, summation general connectivity index, atomic bond connectivity index, geometric arithmetic index, fifth class of geometric arithmetic indices, hyperzagreb index.

**2.1. Molecular characteristics of the linear [n]-pentacene hexane para-line graphs.** Figure 3 depicts the linear [n]-pentacene molecular graph, which is indicated by the symbol  $T_n$ .  $T_n$  consists of  $84n - 6$  edges and  $66n$  vertices.

**Theorem 2.1.** Consider a hexane para-line graphs  $G$  derived from the graph  $T_n$ .

$$M_\alpha(G^*) = (9n + 6)6^{\alpha+6} + 7^{\alpha+5}(36n - 12).$$

**Proof.** In Figure 3, the graph  $G$  is displayed. There are  $168n - 12$  vertices in total in  $G$ , this has  $108n - 36$  vertices of degree and  $60n + 24$  vertices of degree 6, where

$$M_\alpha(G) = (9n + 6)6^{\alpha+6} + 7^{\alpha+5}(36n - 12).$$

**Theorem 2.2** Consider a hexane para-line graphs  $G^*$  derived from the graph  $T_n$ .

$$1. R_\alpha(G^*) = (30n + 30)36^\alpha + (60n - 12)42^\alpha + (132n - 48)49^\alpha.$$

$$2. \chi_\alpha(G^*) = (30n + 30)12^\alpha + (60n - 12)13^\alpha + (132n - 48)14^\alpha.$$

$$3. ABC(G) = (45\sqrt{6} + \frac{264}{9})n + 7\sqrt{6} - \frac{96}{7}.$$

$$4. GA(G) = (162 + 24\sqrt{18})n - 18 - \frac{24}{17}\sqrt{18}.$$

**Proof.** The total number of edges in  $G$  is determined by the formula  $222n - 30$ . The edges in  $G$  can be divided into three sets,  $E_1(G)$ ,  $E_2(G^*)$ , and  $E_3(G)$ , which do not intersect with each other. The edge partition  $E_1(G)$  contains  $30n + 30$  edges  $x_1, x_2$ , where  $d_{x_1} = d_{x_2} = 6$ , edge the partition  $E_2(G)$  contains  $60n - 12$  edges  $x_1, x_2$ , where  $d_{x_1} = 6$  and  $d_{x_2} = 7$ , and The edge partition  $E_3(G)$  consists of  $132n - 48$  edges. This partition includes edges  $x_1$  and  $x_2$ , where  $d_{x_1} = d_{x_2} = 7$ . By utilizing we get the required outcomes using formulae (1), (3), (4) and (5).

**Theorem 2.3** Consider a hexane para-line graphs  $G$  derived from the graph  $T_n$ .



FIGURE 5. Linear Pentacene

$$1. ABC_4(G) = (\sqrt{330} + 12\sqrt{6} + 6\sqrt{90} + \frac{48}{7})n + \frac{9}{6} + \frac{6}{9}\sqrt{105} - \frac{24}{9}\sqrt{6} - \frac{6}{7}\sqrt{90} - \frac{1}{9}\sqrt{330} - \frac{96}{27}$$

$$2. GA_5(G) = (90 + \frac{240}{39}\sqrt{30} + \frac{864}{51}\sqrt{6})n - 6 + \frac{48}{27}\sqrt{9} - \frac{48}{39}\sqrt{30} - \frac{288}{51}\sqrt{6}$$

**Proof.** Assuming that the set of edges depends on the sum of the degrees of the neighbors of the end vertices, we can partition edges that divide  $(G^*)$  into seven distinct sets:  $E_{12}(G)$ ,  $E_{13}(G)$ , ...,  $E_{18}(G)$ . Thus, we have  $E(G) = \bigcup_{i=12}^{18} E_i(G)$ . The edge assortment  $E_{12}(G)$  comprises 18 edges  $x_1x_2$ , where  $S_{x_1} = S_{x_2} = 12$ , the edge collection  $E_{13}(G)$  holds 12 edges  $x_1x_2$ , where  $S_{x_1} = 12$  and  $S_{x_2} = 13$ , the edge collection  $E_{14}(G)$  holds  $18n - 12$  edges  $x_1x_2$ , where  $S_{x_1} = S_{x_2} = 13$ , set of edges  $E_{15}(G)$  contains  $36n - 12$  edges  $x_1x_2$ , where  $S_{x_1} = 13$  and  $S_{x_2} = 16$ , edge the collection  $E_{16}(G)$  contains  $16n$  edges  $x_1x_2$ , where  $S_{x_1} = S_{x_2} = 16$ , the edge set  $E_{17}(G)$  contains  $48n - 16$  edges  $x_1x_2$ ,

where  $S_{x_1} = 16$  and  $S_{x_2} = 17$  and the set of edges  $E_{18}(G)$  is satisfied  $20n - 16$  edges  $x_1x_2$ , where  $S_{x_1} = S_{x_2} = 17$ . By utilizing we can get the required outcomes using formulae 6 and 7.

**Theorem 2.4** Consider a hexane para-line graphs  $G$  derived from the graph  $T_n$

1.  $HM(G) = 40332n - 2412$ .
2.  $PM_1(G) = 12^{30n+30} \times 13^{60n-12} \times 14^{132n-24}$ .
3.  $PM_2(G) = 36^{30n+30} \times 42^{60n-12} \times 49^{132n-24}$ .

**Proof.** Consider a hexane para-line graphs  $G$  of a linear pentacene. Based on the angles of the final vertex, the collection of edges  $E(G)$  might be categorised as three distinct groups. The first category,  $E_1(G)$ , consists of  $30n + 30$  edges  $x_1x_2$ , where  $d_{x_1} = d_{x_2} = 6$ . The second category,  $E_2(G)$ , includes  $60n - 12$  edges  $x_1x_2$ , where  $d_{x_1} = 6$  and  $d_{x_2} = 7$ . The third category,  $E_3(G)$ , comprises  $132n - 24$  edges  $x_1x_2$ , where  $d_{x_1} = d_{x_2} = 7$ . Let  $|E_1(G)| = e_{6,6}$ ,  $|E_2(G)| = e_{6,7}$ , and  $|E_3(G)| = e_{7,7}$ . Therefore,

$$\begin{aligned}
 1. \quad HM(G) &= \sum_{x_1x_2 \in E(G)} (d_{x_1} + d_{x_2})^2 \\
 HM(G) &= \sum_{x_1x_2 \in E_1(G)} [d_{x_1} + d_{x_2}]^2 + \sum_{x_1x_2 \in E_2(G)} [d_{x_1} + d_{x_2}]^2 + \sum_{x_1x_2 \in E_3(G)} [d_{x_1} + d_{x_2}]^2 \\
 HM(G) &= 144|E_1(G)| + 169|E_2(G)| + 196|E_3(G)| \\
 HM(G) &= 144(30n + 30) + 169(60n - 12) + 196(132n - 24) \\
 HM(G) &= 4320n + 4320 + 10140n - 2028 + 25872n - 4704
 \end{aligned}$$

This implies that

$$HM(G) = 40332n - 2412.$$

$$\begin{aligned}
 2. \quad PM_1(G) &= \prod_{x_1x_2 \in E_1(G)} (d_{x_1} + d_{x_2}) \times \prod_{x_1x_2 \in E_2(G)} (d_{x_1} + d_{x_2}) \times \prod_{x_1x_2 \in E_3(G)} (d_{x_1} + d_{x_2}) \\
 PM_1(G) &= 12^{|E_1(G)|} \times 13^{|E_2(G)|} \times 14^{|E_3(G)|} \\
 PM_1(G) &= 12^{30n+30} \times 13^{60n-12} \times 14^{132n-24}. \\
 3. \quad PM_2(G) &= \prod_{x_1x_2 \in E_1(G)} (d_{x_1} \times d_{x_2}) \times \prod_{x_1x_2 \in E_2(G)} (d_{x_1} \times d_{x_2}) \times \prod_{x_1x_2 \in E_3(G)} (d_{x_1} \times d_{x_2}) \\
 PM_2(G) &= 36^{|E_1(G)|} \times 42^{|E_2(G)|} \times 49^{|E_3(G)|} \\
 PM_2(G) &= 36^{|E_1(G)|} \times 42^{|E_2(G)|} \times 49^{|E_3(G)|} \\
 PM_2(G) &= 36^{30n+30} \times 42^{60n-12} \times 49^{132n-24}.
 \end{aligned}$$

**Theorem 2.5** Consider a hexane para-line graphs  $G^*$  derived from the graph  $T_n$

1.  $M_1(G, p) = (30n + 30)P^{12} + (60n - 12)P^{13} + (132n - 24)P^{14}$ .
2.  $M_2(G, p) = (30n + 30)P^{36} + (60n - 12)P^{42} + (132n - 24)P^{49}$ .

**Proof.** 1.  $M_1(G, p) = \sum_{x_1x_2 \in E(G)} P^{(d_{x_1} + d_{x_2})}$

$$M_1(G, p) = \sum_{x_1 x_2 \in E_1(G)} P^{(d_{x_1} + d_{x_2})} + \sum_{x_1 x_2 \in E_2(G)} P^{(d_{x_1} + d_{x_2})} \sum_{x_1 x_2 \in E_1(G)} P^{(d_{x_1} + d_{x_2})}$$

$$M_1(G, p) = \sum_{x_1 x_2 \in E_1(G)} P^{12} + \sum_{x_1 x_2 \in E_2(G)} P^{13} + \sum_{x_1 x_2 \in E_1(G)} P^{14}$$

$$M_1(G, p) = |E_1(G)|P^{12} + |E_2(G)|P^{13} + |E_3(G)|P^{14}$$

$$M_1(G, p) = (30n + 30)P^{12} + (60n - 12)P^{13} + (132n - 24)P^{14}.$$

$$2. M_2(G, p) = \sum_{x_1 x_2 \in E(G)} P^{(d_{x_1} + d_{x_2})}$$

$$M_2(G, p) = \sum_{x_1 x_2 \in E_1(G)} P^{(d_{x_1} \times d_{x_2})} + \sum_{x_1 x_2 \in E_2(G)} P^{(d_{x_1} \times d_{x_2})} \sum_{x_1 x_2 \in E_1(G)} P^{(d_{x_1} \times d_{x_2})}$$

$$M_2(G, p) = \sum_{x_1 x_2 \in E_1(G)} P^{36} + \sum_{x_1 x_2 \in E_2(G)} P^{42} + \sum_{x_1 x_2 \in E_1(G)} P^{49}$$

$$M_2(G, p) = |E_1(G)|P^{36} + |E_2(G)|P^{42} + |E_3(G)|P^{49}$$

$$M_2(G, p) = (30n + 30)P^{36} + (60n - 12)P^{42} + (132n - 24)P^{49}.$$

This makes the proof whole.



FIGURE 6. Hexane para-line graphs linear Pentacene

**2.2. Molecular descriptors of hexane para-line graphs for multiple pentacenes.** The chemical diagram  $T_{m,n}$  representing multiple pentacene is depicted in Figure 4. This graph consists of  $66mn$  vertices and  $99mn - 6m - 9n$  edges.

**Theorem 2.6** Consider a hexane para-line graphs  $G^*$  derived from the graph  $T_{m,n}$ .

$$M\alpha(G) = (9n + 6)6^{\alpha+6} + 7^{\alpha+5}(36n - 12).$$

**Proof.** Figure 5 shows the graph  $G^*$  in a visual format. It has  $168n - 12$  worth of vertices in total, of which  $60n + 24$  and  $108n - 36$  have degrees of 6 and 7, respectively. Using formula 2, we can calculate  $M\alpha(G)$ .

**Theorem 2.7** Consider a hexane para-line graphs  $G$  derived from the graph  $T_{m,n}$ .

$$1. R_\alpha(G) = (10n + 6m + 4)36^\alpha + (4m + 20n - 8)42^\alpha + (99mn - 20m - 55n + 4)49^\alpha.$$

$$2. \chi_\alpha(G) = (10n + 6m + 4)12^\alpha + (4m + 20n - 8)13^\alpha + (99mn - 20m - 55n + 4)14^\alpha.$$

$$3. ABC(G) = (9\sqrt{6} - \frac{330}{7})n + (9\sqrt{6} - \frac{120}{7})m6\sqrt{6} + 198mn + \frac{24}{7}.$$

**Proof.** The division graph  $S(T_{m,n})$  comprises a total of  $198mn - 20m - 50$  vertices and  $99mn - 10m - 25n$  edges. There are  $8m + 20n$  vertices of degree 2 and  $66mn - 12m - 30n$  vertices of degree 3, according to the vertex division. The edge set  $E(G)$  of the hexane para-line graphs  $E(G)$  consists of  $99mn - 20m - 55n + 4$  edges. Based on the angles of the end vertices, these edges



are divided into three groups, i.e.,  $E(G) = E_1(G) \cup E_2(G) \cup E_3(G)$ . The edge separation  $E_1(G)$  consists of  $10n + 6m + 4$  edges  $x_1x_2$ , where  $d_{x_1} = d_{x_2} = 4$ . Edge Separation  $4m + 20n - 8$  with  $E_2(G)$  Edge  $x_1x_2$ , where  $d_{x_1} = 4$  and  $d_{x_2} = 5$ . Lastly, Separating the edges  $E_3(G)$  comprises  $99mn - 20m - 55n + 4$  edges  $x_1x_2$ , where  $d_{x_1} = d_{x_2} = 5$ . By applying the required outcome may be produced using formulae (1), (3), (4) and (5).

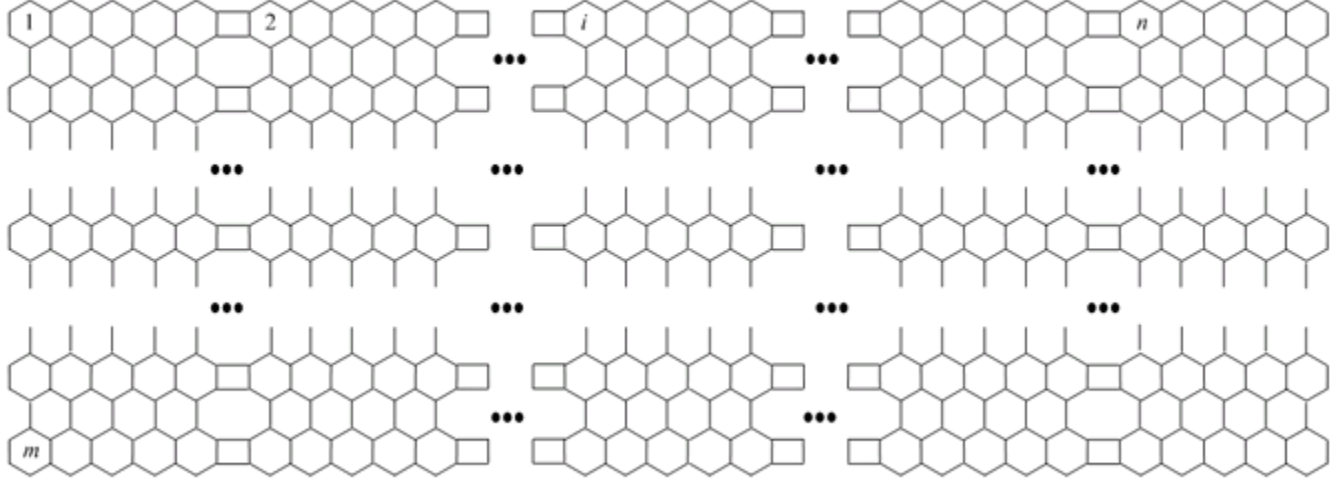


FIGURE 7. Multiple pentacene

**Theorem 2.8** Consider a hexane para-line graphs  $G$  derived from the graph  $T_{m,n}$ .

1.  $ABC_4(G) = (44m + \sqrt{14} + 4\sqrt{2} + \sqrt{110} + 2\sqrt{30} - \frac{116}{3})n + (\frac{1}{2}\sqrt{6} + \frac{1}{5}\sqrt{110} + \frac{2}{5}\sqrt{35} - \frac{112}{9} + \frac{2}{3}\sqrt{30})m + 2\sqrt{6} - \frac{8}{5}\sqrt{2} - \frac{2}{5}\sqrt{110} - \frac{4}{3}\sqrt{30} + \frac{80}{9}$ .
2.  $GA_5(G) = (\frac{80}{13}\sqrt{10} + 99m + \frac{288}{17}\sqrt{269})n + (-26 + \frac{16}{13}\sqrt{10} + \frac{16}{9}\sqrt{5} + \frac{96}{17}\sqrt{2})m - \frac{192}{17}\sqrt{10} - \frac{32}{13}\sqrt{10} + 24$

**Proof.** Seven distinct edge sets may be formed from the set of edges by taking into account the degree sum of end vertices' neighbours.  $E_i(G)$ , where  $i = 6, 7, \dots, 12$ . Thus, we have  $E(G^*) = \bigcup_{i=6}^{12} E_i(G)$ . The edge partition  $E_6(G)$  contains  $2m + 8$  edges  $x_1x_2$ , where  $S_{x_1} = S_{x_2} = 6$ . The edge partition  $E_7(G)$  consists of  $4m$  edges  $x_1x_2$ , where  $S_{x_1} = 6$  and  $S_{x_2} = 7$ . Edge partition  $E_8(G)$  contains  $10n - 4$  edges  $x_1x_2$ , where  $S_{x_1} = S_{x_2} = 7$ . Edge partition  $E_9(G)$  contains  $20n + 4m - 8$  edges  $x_1x_2$ , where  $S_{x_1} = 8$  and  $S_{x_2} = 9$ . Edge partition  $E_{10}(G)$  consists of  $10n$  edges  $x_1x_2$ , where  $S_{x_1} = S_{x_2} = 9$ . Edge partition  $E_{11}(G)$  contains  $8m + 24n - 16$  edge  $x_1x_2$ , where  $S_{x_1} = 10$  and  $S_{x_2} = 11$ . Finally, edge partition  $E_{12}(G)$  contains  $99mn - 28m - 87n + 20$  edge  $x_1x_2$ , where  $S_{x_1} = S_{x_2} = 11$ . By utilizing formulas (6) and (7), we obtain the desired result.

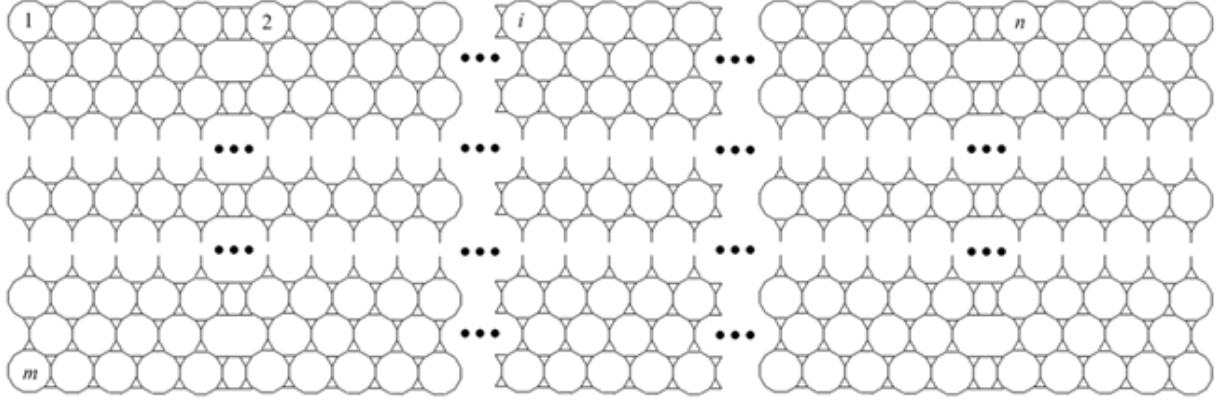


FIGURE 8. Hexane para-line graph multiple of pentacene

By performing computations on the chemical structures of multiple-pentacene, we obtain the following indices:  $HM(G), PM_1(G), PM_2(G)$ .

**Theorem 2.9** Consider a hexane para-line graphs  $G^*$  derived from the graph  $T_{m,n}$ .

1.  $HM(G) = 4851mn - 598m - 1495n4$ .
2.  $PM_1(G) = 12^{10n+6m+4} \times 13^{4m+20n-8} \times 14^{99mn-20m-55n+4}$ .
3.  $PM_2(G) = 36^{10n+6m+4} \times 42^{4m+20n-8} \times 47^{99mn-20m-55n+4}$ .
4.  $M_1(G, p) = (10n + 6m + 4)P^{12} + (4m + 20n - 8)P^{13} + (99mn - 20m - 55n + 4)P^{14}$ .
5.  $M_2(G, p) = (10n + 6m + 4)P^{36} + (4m + 20n - 8)P^{42} + (99mn - 20m - 55n + 4)P^{49}$ .

**Proof.** Consider a graph  $G$  with its edges broken down into three parts categories due to the degrees of the final vertex. The initial category, denoted as  $E_1(G)$ , consists of  $10n + 6m + 4$  edges  $x_1x_2$ , which both vertices  $x_1$  and  $x_2$  have a degree of 6. The second category, denoted as  $E_2(G)$ , contains  $4m + 20n - 8$  edges  $x_1x_2$ , which  $x_1$  has a degree of 6 and  $x_2$  has a degree of 7. The third category, denoted as  $E_3(G)$ , includes  $99mn - 20m - 55n + 4$  edges  $x_1x_2$ , where both vertices  $x_1$  and  $x_2$  have a degree of 7. We can observe that the cardinality of  $E_1(G)$  is equal to  $e_{6,6}$ ,  $E_2(G)$  is equal to  $e_{6,7}$  and  $E_3(G)$  is equal to  $e_{7,7}$ .

$$1. HM(G) = \sum_{x_1x_2 \in E(G)} (d_{x_1} + d_{x_2})^2$$

$$HM(G) = \sum_{x_1x_2 \in E_1(G)} [d_{x_1} + d_{x_2}]^2 + \sum_{x_1x_2 \in E_2(G)} [d_{x_1} + d_{x_2}]^2 + \sum_{x_1x_2 \in E_3(G)} [d_{x_1} + d_{x_2}]^2$$

$$HM(G) = 36|E_1(G)| + 42|E_2(G)| + 49|E_3(G)|$$

$$HM(G) = 36(10n + 6m + 4) + 42(4m + 20n - 8) + 49(99mn - 20m - 55n + 4)$$

$$HM(G) = 360n + 216m + 144 + 168m + 840n - 336 + 4851mn - 980m - 2695n + 196$$

This implies that

$$HM(G) = 4851mn - 598m - 1495n4$$

Since,

$$\mathbf{2.} \quad PM_1(G) = \prod_{x_1x_2 \in E(G)} (d_{x_1} + d_{x_2})$$

$$PM_1(G) = \prod_{x_1x_2 \in E_1(G)} (d_{x_1} + d_{x_2}) \times \prod_{x_1x_2 \in E_2(G)} (d_{x_1} + d_{x_2}) \times \prod_{x_1x_2 \in E_3(G)} (d_{x_1} + d_{x_2})$$

$$PM_1(G) = 12^{10n+6m+4} \times 13^{4m+20n-8} \times 14^{99mn-20m-55n+4}.$$

Now that

$$\mathbf{3.} \quad PM_2(G) = \prod_{x_1x_2 \in E(G)} (d_{x_1} \times d_{x_2})$$

$$PM_2(G) = \prod_{x_1x_2 \in E_1(G)} (d_{x_1} \text{ times } d_{x_2}) \times \prod_{x_1x_2 \in E_2(G)} (d_{x_1} \times d_{x_2}) \times \prod_{x_1x_2 \in E_3(G)} (d_{x_1} \times d_{x_2})$$

$$PM_2(G) = 36^{|E_1(G)|} \times 42^{|E_1(G)|} \times 49^{|E_1(G)|}$$

$$PM_2(G) = 36^{10n+6m+4} \times 42^{4m+20n-8} \times 49^{99mn-20m-55n+4}.$$

$$\mathbf{4.} \quad M_1(G, p) = \sum_{x_1x_2 \in E(G)} P^{(d_{x_1}+d_{x_2})}$$

$$M_1(G, p) = \sum_{x_1x_2 \in E_1(G)} P^{(d_{x_1}+d_{x_2})} + \sum_{x_1x_2 \in E_2(G)} P^{(d_{x_1}+d_{x_2})} \sum_{x_1x_2 \in E_1(G)} P^{(d_{x_1}+d_{x_2})}$$

$$M_1(G, p) = \sum_{x_1x_2 \in E_1(G)} P^{12} + \sum_{x_1x_2 \in E_2(G)} P^{13} + \sum_{x_1x_2 \in E_1(G)} P^{14}$$

$$M_1(G, p) = |E_1(G)|P^{12} + |E_2(G)|P^{13} + |E_3(G)|P^{14}$$

$$M_1(G, p) = (10n + 6m + 4)P^{12} + (4m + 20n - 8)P^{13} + (99mn - 20m - 55n + 4)P^{14}.$$

$$\mathbf{5.} \quad M_2(G, p) = \sum_{x_1x_2 \in E(G)} P^{(d_{x_1} \times d_{x_2})}$$

$$M_2(G, p) = \sum_{x_1x_2 \in E_1(G)} P^{(d_{x_1} \times d_{x_2})} + \sum_{x_1x_2 \in E_2(G)} P^{(d_{x_1} \times d_{x_2})} \sum_{x_1x_2 \in E_1(G)} P^{(d_{x_1} \times d_{x_2})}$$

$$M_2(G, p) = \sum_{x_1x_2 \in E_1(G)} P^{36} + \sum_{x_1x_2 \in E_2(G)} P^{42} + \sum_{x_1x_2 \in E_1(G)} P^{49}$$

$$M_2(G, p) = |E_1(G)|P^{36} + |E_2(G)|P^{42} + |E_3(G)|P^{49}$$

$$M_2(G, p) = (10n + 6m + 4)P^{36} + (4m + 20n - 8)P^{42} + (99mn - 20m - 55n + 4)P^{49}.$$

This makes the proof whole.

### 3. CONCLUSION

The research article examined mathematical indices essential to chemical informatics, specifically used in analyzing organic compounds. These indices include the randic general connectivity index, first zagreb general index, summation general connectivity index, atomic bond connectivity index, geometric arithmetic index, fifth class of geometric arithmetic indices, hyper zagreb index, as well as the initial and secondly multiple [n]-pentacene zagreb indices. The focus of our investigation involved heptane para-line graphs associated with two distinct types of pentacenes. The randic index ( $R_\alpha$ ) is a useful tool for understanding alkane physicochemical properties, while the ABC index predicts hydrocarbon stability for linear and branched alkanes. Cycloalkane stability can be assessed using this index, providing valuable insights. The GA index outperforms the ABC index in predicting physicochemical characteristics, chemical reactivity, and biological activities of pentacenes, enhancing our understanding through a philosophical approach. The study indicates that physical features can be linked to pentacenes' chemical structure, potentially benefiting the power industry and advancing advancements in the field.

### REFERENCES

- [1] Li X., Shi Y., A survey on the Randic' index, MATCH Commun. Math. Comput. Chem. (2008), 59(1), 127-156. DOI: 10.46793/match.90-2.495L.
- [2] Li X., Shi Y., Wang L., An updated survey on the Randic' index, in: B.F. I. Gutman (Ed.), Recent Results in the Theory of Randic Index, University of Kragujevac and Faculty of Science Kragujevac, (2008), 9-47.
- [3] Mufti Z.S., Zafar S., Zahid Z., Nadeem M. F., Study of the paraline graphs of certain Benzenoid structures using topological indices. MAGNT Research Report, (2017), 4(3), 110-116.
- [4] Rada J., Cruz R., Vertex-degree-based topological indices over graphs, MATCH Commun. Math. Comput. Chem. (2014), 72, 603- 616. DOI: 10.1007/s10910-011-9876-6.
- [5] Hinz A.M., Parisse D., The average eccentricity of Sierpiński graphs, Graphs and Combinatorics, (2012), 28(5), 671-686. DOI: 10.1007/s00373-011-1076-4.
- [6] Devillers J., Balaban A.T., Topological indices and related descriptors in QSAR and QSPAR. CRC Press, (2000).
- [7] Azari M., Iranmanesh A., Harary index of some nano-structures, MATCH Commun. Math. Comput. Chem., (2014), 71, 373-382. DOI: 10.46793/match.90-2.495L.
- [8] Feng L., Liu W., Yu G., Li S., The hyper-Wiener index of graphs with given bipartition, Utilitas Math. (2014), 95, 23-32, Utilitas Mathematica 95:23-32.
- [9] Ali A., Nazeer W., Munir M., Kang S.M., M-Polynomials and Topological Indices Of Zigzag and Rhombic Benzenoid Systems. Open Chemistry, (2018), 16(1), 73-78. DOI: 10.1515/chem-2018-0010.
- [10] Knor M., Lužar B., Škrekovski R., Gutman I., On Wiener index of common neighborhood graphs, MATCH Commun. Math. Comput. Chem., (2014), 72, 321-332. DOI: 10.46793/match.90-2.495L.
- [11] Xu K., Liu M., Das K., Gutman I., Furtula B., A survey on graphs extremal with respect to distance-based topological indices, MATCH Commun. Math. Comput. Chem. (2014), 71, 461-508. DOI: 10.46793/match.90-2.495L.
- [12] Schultz H.P., Topological organic chemistry, Graph theory and topological indices of alkanes. Journal of Chemical Information and Computer Sciences, (1989), 29(3), 227-228. DOI: 10.1021/ci9800312.
- [13] Xu K., Das K.C., Liu H., Some extremal results on the connective eccentricity index of graphs. Journal of Mathematical Analysis and Applications, (2016), 433(2), 803-817. DOI: 10.1016/j.jmaa.2015.08.027.

- [14] Kanna M.R., Jagadeesh R., Topological Indices of Vitamin A., *Int. J. Math. And Appl.*, (2018), 6(1B), 271-279. DOI: 10.3934/math.2022999.
- [15] Virk A., Nazeer W., Kang S.M., On Computational Aspects of Bismuth Tri-Iodide., *Preprints*, (2018), 2018060209. doi: 10.20944/preprints201806.0209.v1.
- [16] Dehmer M., Emmert-Streib F., Grabner M., A computational approach to construct a multivariate complete graph invariant, *Inform. Sci.* (2014), 260, 200-208. DOI: 10.1016/j.ins.2013.11.008.
- [17] Feng L., Liu W., Ilic' A., Yu G., The degree distance of unicyclic graphs with given matching number, *Graphs Comb.*, (2013), 29, 449-462, DOI: 10.1007/s00373-015-1527-4.
- [18] Gutman I., Selected properties of the Schultz molecular topological index, *J. Chem. Inf. Comput. Sci.*, (1994), 34, 1087-1089.
- [19] Farahani M. R., Nadeem M. F., Zafar S., , Zahid Z., , Husin M. N., Study of the topological indices of the line graphs of hpantacenic nanotubes. *New Front. Chem.*, (2017), 26(1), 31-38.
- [20] Soleimani N., Mohseni E., Maleki N., Imani N., Some topological indices of the family of nanostructures of polycyclic aromatic hydrocarbons (PAHs). *J. Natl. Sci Found. Sri.*, (2018), 46(1). DOI: 10.4038/jnsfsr.v46i1.8267.
- [21] Soleimani N., Nikmehr M.J., Tavallaee H.A., Theoretical study of nanostructures using topological indices. *Stud. U. Babes-Bol, Che.*, (2014), 59(4), 139-148.
- [22] Li X., Zhao H., Trees with the first three smallest and largest generalized topological indices, *MATCH Commun. Math. Comput. Chem.*, (2004), 50, 57-62.
- [23] Zhou B., Trinajstić N., On general sum-connectivity index, *J. Math. Chem.*, (2010), 47, 210-218.
- [24] Estrada E., Torres L., Rodriguez L., Gutman I., An atom-bond connectivity index: Modelling the enthalpy of formation of alkanes. *Indian J. Chem.*, (1998), 37A, 849-855. DOI: 10.1007/s10910-022-01403-1.
- [25] Vukicevic D., Furtula B., Topological index based on the ratios of geometrical and arithmetical means of end-vertex degrees of edges, *J. Math. Chem.*, (2009), 46, 1369-1376. DOI: 10.1016/j.dam.2011.06.020.
- [26] Ghorbani M., Hosseinzadeh M.A., Computing ABC4index of nanostar dendrimers, *Optoelectron. Adv. Mater.-Rapid Commun.*, (2010), 4(9), 1419-1422, DOI: 10.12732/ijpam.v11i1.10.
- [27] Graovac A., Ghorbani M., Hosseinzadeh M.A., Computing fifth geometric-arithmetic index for nanostar dendrimers, *J. Math. Nanosci.*, (2011), 1, 33-42.
- [28] Ranjini P.S., Lokesh V., Rajan M.A., On the Schultz index of the subdivision graphs, *Adv. Stud. Contemp. Math.*, (2011), 21(3), 279-290.
- [29] Ranjini P.S., Lokesh V., Cangül I.N., On the Zagreb indices of the line graphs of the subdivision graphs, *Appl. Math. Comput.*, (2011), 218, 699-702. DOI: 10.1016/j.amc.2011.03.125.
- [30] Su G., Xu L., Topological indices of the line graph of subdivision graphs and their Schur-bounds, *Appl. Math. Comput.*, (2015), 253, 395-401.
- [31] A. Asghar, A. Qayyum and N. Muhammad, Different Types of Topological Structures by Graphs, *European Journal of Mathematical Analysis*, 3(2022), DOI:10.12691/ajma-10-1-2.
- [32] Zaib Hassan Niazi, Muhammad Awais Tariq Bhatti, Muhammad Aslam, Yasir Qayyum, Muhammad Ibrahim, Ather Qayyum , d -Lucky Labelling of Some Special Graphs, *American Journal of Mathematical Analysis*, 10;1 (2022), DOI: 10.12691/ajma-10-1-2.
- [33] Mukhtar Ahmad, Saddam Hussain, Iqra Zahid, Ulfat parveen, Muhammad Sultan and Ather Qayyum "On degree based topological indices of petersen subdivision graph", *European Journal of Mathematical Analysis*. 3

(2023) 20, doi: 10.28924/ada/ma.3.20.

- [34] Mukhtar Ahmad, Muhammad Jafar Hussain, Gulnaz Atta, Sajid Raza, Irfan Waheed, Ather Qayyum, "Topological Evaluation of Four Para-Line Graphs Absolute Pentacene Graphs Using Topological", International Journal of Analysis and Applications (2023), 21:0, <https://doi.org/10.28924/2291-8639-21-2023-0>.